INTENTIONALLY LEFT BLANK

4. USE OF COMPUTER SOFTWARE

This document provides a summary of several calculations, as described in Section 1, in which software was utilized to derive the results summarized here. In this present calculation, only the UDEC software was used to develop new results not previously reported in supporting calculations. The computer software used to develop results summarized in this calculation, but developed in the supporting calculations is also reviewed in this section for completeness. The computer software cited in Section 4 of the supporting structural calculations (BSC 2003 [DIRS 167083]; BSC 2004 [DIRS 168993]; and BSC 2004 [DIRS 170791]) is also listed in Table 4-1.

Table 4-1. Computer Software Used in Structural Calculations

Software	STN	Operating system	Computer Type	Computer Number[a]
ANSYS V5.6.2 (BSC 2002 [DIRS 159357])	10364-5.6.2-01	HP-UX 11.00	Hewlett-Packard (HP) 9000 series UNIX workstations	117162, 151324, 151325, 151664, and 151665
LS-DYNA V960.1106 (BSC 2002 [DIRS 158898])	10300-960.1106-00	HP-UX 11.00	HP 9000 series UNIX workstation	117162, 151324, 151325, 151665, 151664, 150691, 150689, 150690, 150688
LS-DYNA V970.3858 D MPP-00 (BSC 2003 [DIRS 166918])	10300-970.3858 D MPP-00	HP-UX 11.22	HP Itanium2 (IA64) series UNIX workstations	501711
UDEC V3.1 (BSC 2002 [DIRS 161949])	10173-3.1-00	Windows 2000	PC	NA
TrueGrid V2.1.5	exempt of the requirements defined in LP-SI.11Q-BSC (Section 2.1.2)	HP-UX 11.00	HP 9000 series UNIX workstation	150689
TrueGrid V2.2	exempt of the requirements defined in LP-SI.11Q-BSC (Section 2.1.2)	HP-UX 11.00	HP 9000 series UNIX workstation	150689
LSPOST V2	exempt of the requirements defined in LP-SI.11Q-BSC (Section 2.1.2)	HP-UX 11.00	HP 9000 series UNIX workstation	117162, 151324, 151325, 151665, 151664, 150691, 150689, 150690, 150688
LS-PREPOST V1.0	exempt of the requirements defined in LP-SI.11Q-BSC (Section 2.1.2)	HP-UX 11.22	HP Itanium2 (IA64) series UNIX workstations	501711
LS-PREPOST V2.0	exempt of the requirements defined in LP-SI.11Q-BSC (Section 2.1.2)	HP-UX 11.22	HP Itanium2 (IA64) series UNIX workstations	501711

[a] Yucca Mountain Project property tag numbers for computers located in Las Vegas, Nevada.

The FE meshes of the DS developed in the supporting calculations were constructed using either ANSYS V5.6.2 (BSC 2002 [DIRS 159357]) or TrueGrid V2.1.5 and TrueGrid V2.2 (XYZ Scientific Applications, Inc.). These software programs were used solely to mesh geometric representations of the domain (i.e., for the development of FE mesh), and are therefore exempt from the requirements defined in procedure LP-SI.11Q-BSC, which defines software qualification requirements.

The qualified FE analysis computer codes used for this calculation are Livermore Software Technology Corporation LS-DYNA V960.1106 (BSC 2002 [DIRS 158898]) and LS-DYNA V970.3858 D MPP-00 (BSC 2003 [DIRS 166918]) (LS-DYNA V960 and LS-DYNA V970, respectively[4]). Both LS-DYNA codes are obtained from Software Configuration Management in accordance with the appropriate procedure (LP-SI.11Q-BSC). The FE calculations performed herein are fully within the range of the validation performed for LS-DYNA V960 code (BSC 2002 [DIRS 168545], Sections 4 and 5) and LS-DYNA V970 code (DOE 2003 [DIRS 168558], Sections 4 and 5). LSPOST V2, LS-PREPOST V1.0 and LS-PREPOST V2.0 (Livermore Software Technology Corporation) are postprocessors[5] used for visual display and graphical representation of results.

The qualified DE analysis computer code used for this calculation is UDEC (BSC 2002 [DIRS 161949]). UDEC is obtained from Software Configuration Management in accordance with the appropriate procedure (LP-SI.11Q-BSC). The DE calculations performed herein are fully within the range of the validation performed (BSC 2002 [DIRS 171617]).

The data files and saved file states to recreate the parametric kinematic analyses conducted with UDEC V3.1 are provided in Attachment A. Files for each case listed in Table 5-19 are reviewed in Section 7 of this document and provided in Attachment I. The file extensions have the following meaning: *.dat are primary input data files, *.fis and *.fin are macro files called by *.dat in setting up and running the problems, *.vel are input velocity ground motion time history records (H signifies horizontal and up signifies vertical velocity components), *.sav are the saved files used for the initial model geometry (before application of the ground motion time histories) and at the end of the analysis.

[4] LS-DYNA V960 and LS-DYNA V970 are referred to as LS-DYNA when it is unnecessary to make a specific distinction.

[5] Note that LS-PREPOST V1.0 and LS-PREPOST V2.0 also have preprocessing capabilities, which were not used in the calculations documented in the supporting calculations.

5. CALCULATION

5.1 BACKGROUND INFORMATION

Figure 5-1 illustrates the major components of the engineered barrier system (EBS) in a typical emplacement drift. The major EBS components are the waste package, the DS, and the fuel rod cladding (the cladding is not shown in Figure 5-1). These components provide barriers to the release of radionuclides from the EBS into the unsaturated zone. The effectiveness of these barriers is potentially compromised by the direct effects from an earthquake, including vibratory ground motion, fault displacement, and rockfall induced by ground motion or some other effects. Other, non-seismic mechanical effects could include rockfall resulting from time-dependent degradation of the emplacement drift. The effectiveness of these barriers is also potentially compromised by indirect effects after an earthquake, including changes in seepage, temperature, and relative humidity if an emplacement drift collapses completely during a very low probability earthquake.

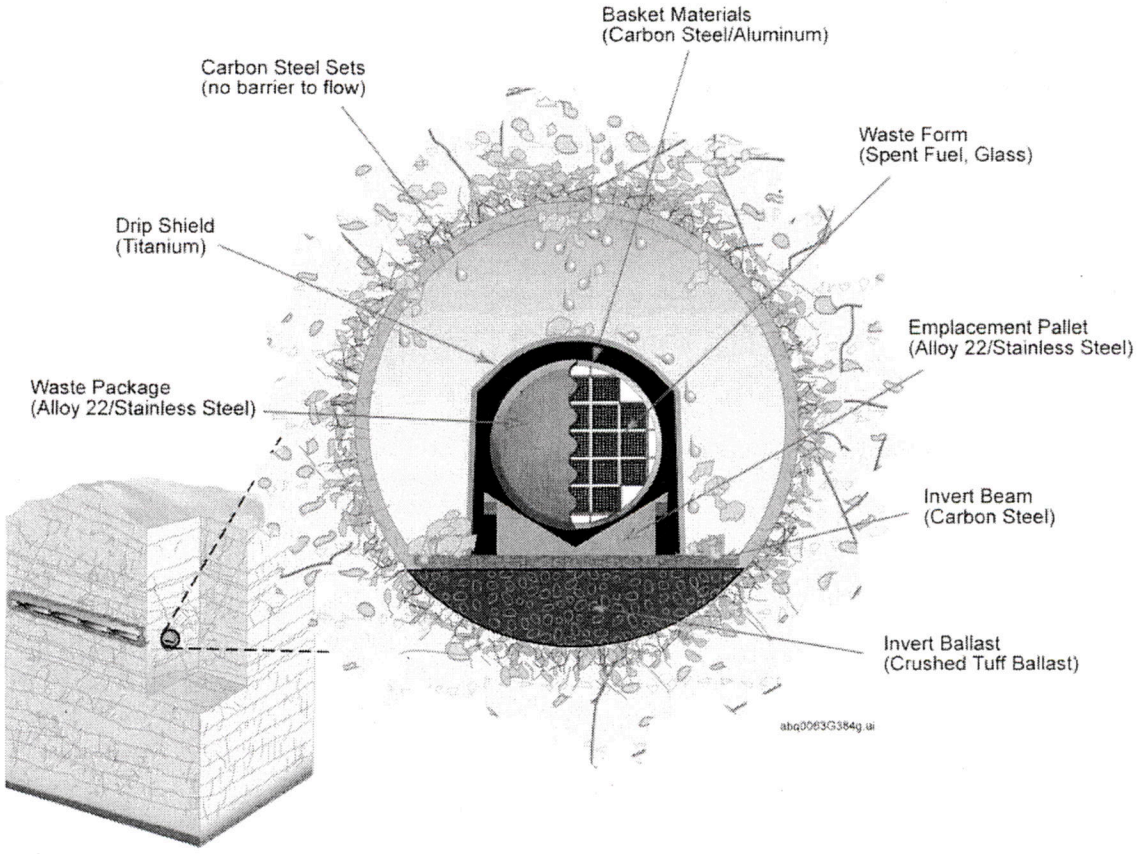

Figure 5-1. Schematic Diagram of the EBS Components in a Typical Emplacement Drift

The DS is a free-standing structure, constructed of titanium bulkheads and overlying sheets, whose legs rest on the invert of the tunnel. The invert is constructed of carbon steel beams with crushed tuff compacted between them. Initially the weight of the DS is borne by the steel beams. As corrosion of these beams occurs over time, the weight will be transferred to the compacted, crushed tuff invert. The purpose of the DS is to prevent direct seepage of water on the waste packages, and to protect the waste packages from direct impacts by rockfall (illustrated in Figure 5-1). Specifically, effectiveness of the DS could be affected by the following mechanical processes:

- Relatively large rigid-body displacements of the DSs that would overturn the DS or create a gap between the neighboring DSs (The DSs are designed to overlap each other creating a continuous shielded area underneath them. This potential separation is an important consideration because it impacts the function of the DS as a flow and rockfall barrier.)

- Loss of structural integrity due to mechanical collapse or buckling of the main structural elements (e.g., the support beam and the bulkhead)

- Puncture, tearing or damage that would accelerate the stress corrosion rate of the DS plates (other corrosion mechanisms are accounted for in the calculation by a uniform thickness reduction of the DS as discussed in Assumption 3.13 and Section 5.2.3.1.5).

The DS could be subjected to static and dynamic loads during the postclosure period. Static load that could potentially have an effect on structural integrity of the DS is due to the weight of caved rock rubble that may rest on the top of the DS or between the DS and the walls of the emplacement drift. Emplacement drift failure, and resulting caving and expansion of the tunnel profile can occur as a result of thermally induced stresses, seismic loading, time-dependent strength degradation, or different combinations of these factors. The dynamic loads on the DS, which are primarily due to the seismic ground motion, include inertial forces and impacts of the falling rock blocks. The inertial forces can result in motion of the DSs relative to each other, and relative to the drift walls and other objects inside the drift (e.g., the waste packages and pallet). Consequently, inertial forces can cause separation of the DSs and impact to other DSs and objects inside the emplacement drifts. The impacts of the falling blocks can take place during seismic ground motion and as a result of drift degradation due to time-dependent strength loss.

The calculations summarized in this document determine potential for separation of the DSs and loss of the structural integrity and stability, but also the damaged areas on the DS (i.e., those areas that exceed the residual stress threshold for Ti-7) from impacts between the DS and the waste package, pallet, invert, drift wall, and by rockfall. The damaged area estimates to the DS surface plates as a function of peak ground velocity (PGV) are used as input to the *Seismic Consequence Abstraction* (BSC 2004 [DIRS 169183]), which provides damage abstractions to the TSPA-LA. In the *Seismic Consequence Abstraction* (BSC 2004 [DIRS 169183]), the physical interpretation of the damaged areas is a resulting network of stress corrosion cracks through which seepage water could potentially pass to the waste package. A discussion of the physical morphology of the stress corrosion cracks, and the potential for advective flux through the DS is provided in the *Seismic Consequence Abstraction* (BSC 2004 [DIRS 169183]).

5.1.1 Scope of Calculation

Integrity and stability of the DS were analyzed for the following loads, which are expected to be the bounding loading cases during the operation of the DS during the postclosure period:

- Static pressure of the rock rubble that covers the DS following collapse or partial collapse from seismic effects or from time-dependent degradation
- Vibratory motion of the DS induced by the seismic ground motion
- Impacts by the falling rock from rockfall due to seismic effects.

5.1.1.1 Loading from Static Pressure of Rock Rubble

Static pressure of rock rubble resting on the DS is derived from two basic sources as described in *Drift Degradation Analysis* (BSC 2004 [DIRS 166107], Section 6.4). These are: 1) low probability seismic events with large peak ground velocity and 2) the combined effects of thermal stresses, time-dependent strength degradation and repeated higher probability seismic events.

Complete or Partial Drift Collapse from Low Probability Seismic Events – Low probability postclosure seismic events are predicted to result in extensive collapse of emplacement drifts in lithophysal rock and partial collapse of nonlithophysal rock, with resulting rubble either completely or partially covering the DS. Drifts located in lithophysal rock are expected to undergo collapse sufficient to cover the DS for seismic events characterized by a PGV of approximately 2 m/s or higher. Approximately 25 percent of the ground motions associated with the 1×10^{-5}, and all of the 1×10^{-6} and lower annual frequency of occurrence show complete collapse in lithophysal rocks. Ground motions associated with 1×10^{-6} and lower annual frequency of occurrence show extensive damage that either covers the DS or fills the area between the DS and drift walls in the nonlithophysal rocks (BSC 2004 [DIRS 166107]). Dynamic discontinuum analyses presented in *Drift Degradation Analysis* (BSC 2004 [DIRS 166107]) show that the collapse of the drifts in response to the ground motion occurs simultaneous with the arrival of the strong ground motion. Thus, within a few seconds after beginning of seismic ground motion, the drift collapses and restrains the DS with broken rubble.

Rockfall from Thermal Stress, Time-Dependent Effects and Higher Probability Seismic Events – In the absence of low probability seismic events, the emplacement drifts are expected to be largely stable over the postclosure period. For the assumed base case scenario (i.e., rock mass loading resulting from thermally induced stresses and higher probability, preclosure ground motions [i.e., those with 5×10^{-4} or 1×10^{-4} annual frequency of occurrence]) some lesser amount of rockfall is expected. This rockfall, derived from the drift sidewalls, will occur primarily in the lithophysal rocks and will vary along the drifts depending on the local quality of the rock mass. The lithophysal rock comprises approximately 85 percent of the total length of the emplacement drifts, while approximately 15 percent occurs within the stronger nonlithophysal rocks. Within the lithophysal rocks and in the absence of low probability seismic events, it is expected that at most, approximately 3 percent of the total length of the emplacement drifts can completely

collapse covering the DS with broken rock[6]. The rockfall along the remaining length of the emplacement drifts will be limited with some accumulation of the broken rock on the sides or on the top (less than 1 m height of the broken rock) of the DS.

5.1.1.2 Loading from Vibratory Motion

The effect of seismic ground motion on damage from vibratory motion of the DS was analyzed for ground motions with 5×10^{-4}, 1×10^{-6} and 1×10^{-7} annual frequency of occurrence. The effect of seismic ground motion on potential for separation of the DSs was analyzed for ground motions with 1×10^{-6} and 1×10^{-7} annual frequency of occurrence. Although the caved rock mass inside the emplacements drifts (surrounding the DS) could potentially restrict motion of the DS as a rigid body, it was assumed conservatively in a number of the calculations that the drifts were stable during the entire simulation (as stated in Section 5.1.1.1, collapse of the drifts in lithophysal rock and nonlithophysal rock masses is expected for seismic ground motions with 1×10^{-6} and 1×10^{-7} annual frequency of occurrence). The seismic motion is transmitted from the invert (which has the identical motion of the far-field rock mass in these calculations – see Section 5.2.3.4) to the DS through the frictional interface in the contacts between the invert and the DS.

5.1.1.3 Loading from Rockfall Impacts

Rockfall, which can occur as gradual drift degradation or can be seismically induced, may impact the DS. The seismically induced impacts of the rockfall, which will have greater energy (because of larger impact velocity) than the impacts resulted from slow, quasi-static drift degradation, are considered in the analysis. The size distribution of the unstable blocks will be different in the lithophysal and nonlithophysal rock masses. Spacing of the rock mass fractures and lithophysae is expected to control the size of the blocks in general, and the size of those blocks that are detached under seismic load. The nonlithophysal rock mass is characterized by four sets of naturally-occurring fractures, with spacings that average, in general, between 0.5 m and 3 m (BSC 2004 [DIRS 166107], Section 6.1). The ubiquitous fracture fabric of relatively short fractures in the lithophysal rock mass have average spacing of less than 0.1 m. The median and maximum block sizes produced in the nonlithophysal rock mass are larger as a result of the wider fracture spacing. The rockfall in lithophysal rock mass is estimated to consist of blocks with edge length of, on average, a few tens of centimeters, in contrast to the largest blocks destabilized by the strong ground motions (1×10^{-6} and 1×10^{-7}) in nonlithophysal rock mass with mass in excess of 25 metric tons. Impact of blocks in nonlithophysal rock mass is analyzed as a bounding scenario in *Drip Shield Structural Response to Rock Fall* (BSC 2004 [DIRS 168993]) and summarized in Section 5.4.2.

[6] The lithophysal rock mass has been subdivided into 5 rock strength categories, with category 1 being of the lowest quality or strength. This category, representative of lithophysal rock with lithophysal porosity greater than about 25 percent comprises roughly 3 percent of the repository host horizon (BSC 2004 [DIRS 166107], Appendix E).

5.2 DRIP SHIELD GEOMETRY

5.2.1 Description of the Drip Shield Design

The geometry of the DS is shown in perspective views in Figures 5-2 and 5-3. All details and dimensions of the geometry of the DS can be found in *D&E / PA/C IED Interlocking Drip Shield and Emplacement Pallet* (BSC 2004 [DIRS 169220]) as well as in the calculations that support this summary document (BSC 2003 [DIRS 163425], BSC 2004 [DIRS 168993] and BSC 2004 [DIRS 170791]). The components of the DS structure are indicated in these figures. The main structural (load bearing) elements of the DS, the bulkheads and the support beams, will be manufactured of Ti-24. They form 4 typical frames spaced at 1,072 mm along the DS. Two peripheral frames (at the ends of the DS) have a different geometry than the bulkhead and support beams. The DS plates 1 (on the top) and 2 (on the sides), which are placed continuously over the bulkheads and the support beams, will be manufactured of Ti-7, as well as the external and internal support plates that strengthen the DS plates 1 and 2 in the region of their junction. The plates provide the ultimate functionality of the structure—i.e., to prevent: a) dripping of water from the drift roof and walls onto the waste packages, and b) impacts of loose blocks from the drift roof and the walls directly onto the waste packages. Each DS is 5,805 mm in length, and 2,886 mm in height, and its total mass is 5,000 kg (BSC 2004 [DIRS 169220]). The DSs will be installed, prior to closure of the repository, over the waste packages and pallets. Adjacent DSs partially overlap one another using the drip shield connector (DSC) assembly on one DS, which is placed over and interlocks the DSC Guide of the next DS to provide continuous shielding of the waste packages. In order to separate (unlock) two DSs (or to lock them together) without significantly deforming the support beams, bulkheads or plates, or shearing off the welds, it is necessary to lift one DS relative to another by at least 40 inches (approximately 1 m; shown in Figure 5-4). This is because the DS side plates are inclined 2 degrees with respect to the invert surface normal (BSC 2004 [DIRS 169220]).

The DS and other structures inside the emplacement drift after its installation are shown in the cross-section in Figure 5-5. The details of the invert structural support for the DS and its relationship to the emplacement drift are shown in Figure 5-6. The DS will be placed between the edge of the pallet (inside) and the gantry crane rail and the associated structures (outside). However, in the calculations, it is assumed (Assumption 3.16) that the gantry crane rail and the associated structure do not exist—i.e., that in the postclosure period they have corroded in such a way that they do not provide any mechanical resistance or obstacle to motion of the DS. The DS will be resting on the invert by its own weight. Initially, the weight of the DS, waste package and pallet is borne by a framework of structural steel that is bolted to the floor of the emplacement drift. Compacted, crushed tuff is placed between the structural steel members during the construction process and prior to emplacement. In the postclosure period, as the steel framework corrodes and looses its load bearing capacity, the weight of the DS, waste package and pallet will be borne by the compacted crushed tuff invert. As shown in Figure 5-6, the maximum thickness of the crushed tuff is approximately 86 mm (2 ft 10 in) beneath the waste package. There is no additional resistance to lifting the DS off the invert than the weight of the DS. The only resistance to lateral movement of the DS (before it hits the pallet or the drift wall) is friction between the DS and the invert.

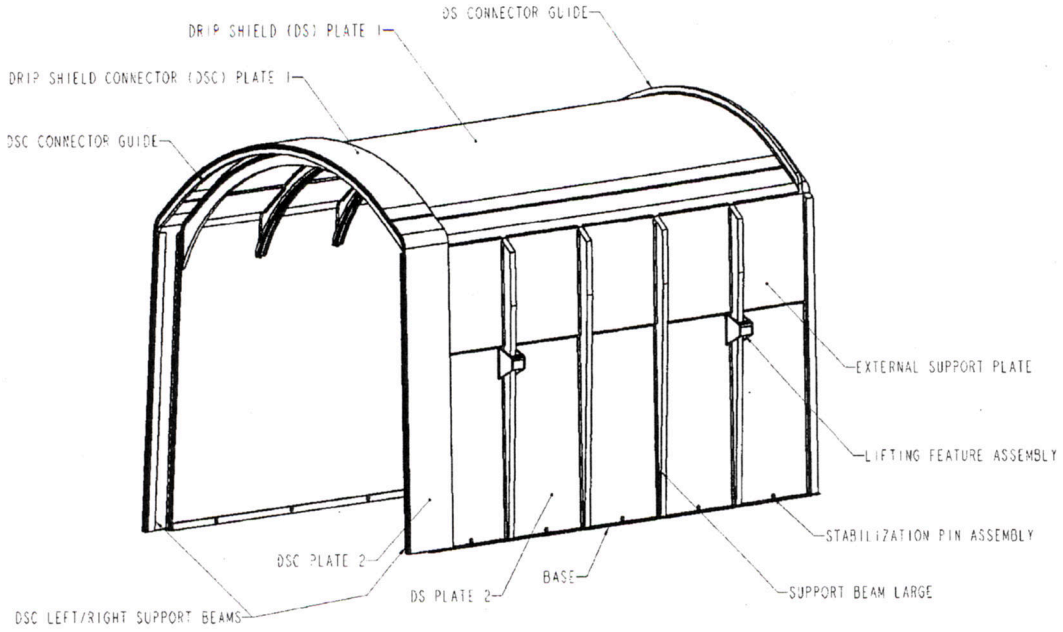

Source: BSC 2004 [DIRS 168275].

Figure 5-2. Geometry of the Drip Shield – Side View

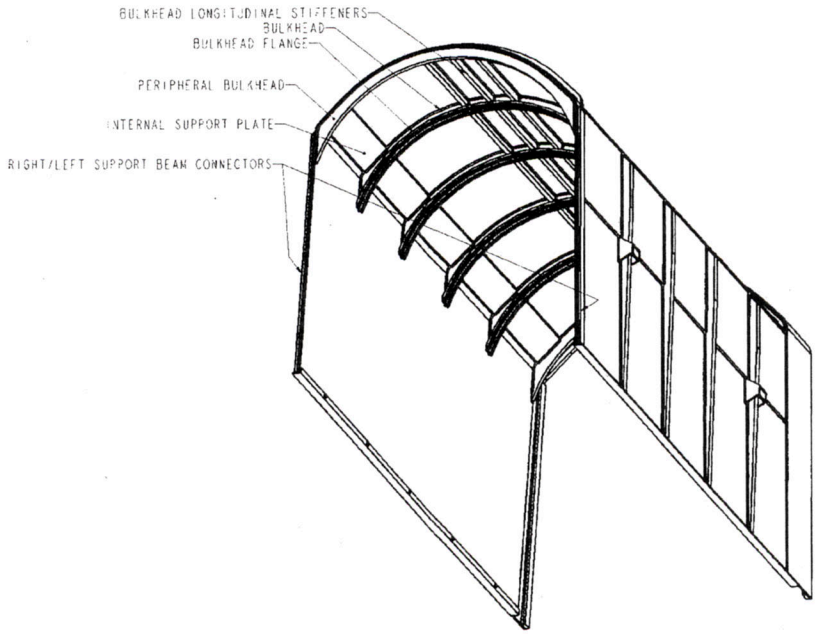

Source: BSC 2004 [DIRS 168275].

Figure 5-3. Geometry of the Drip Shield – View from Below

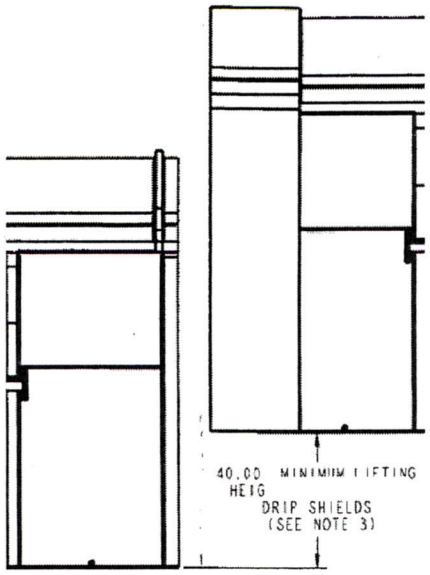

NOTE: The indicated dimension is in inches.

Source: BSC 2003 [DIRS 165038].

Figure 5-4. Interlocking of the Drip Shields

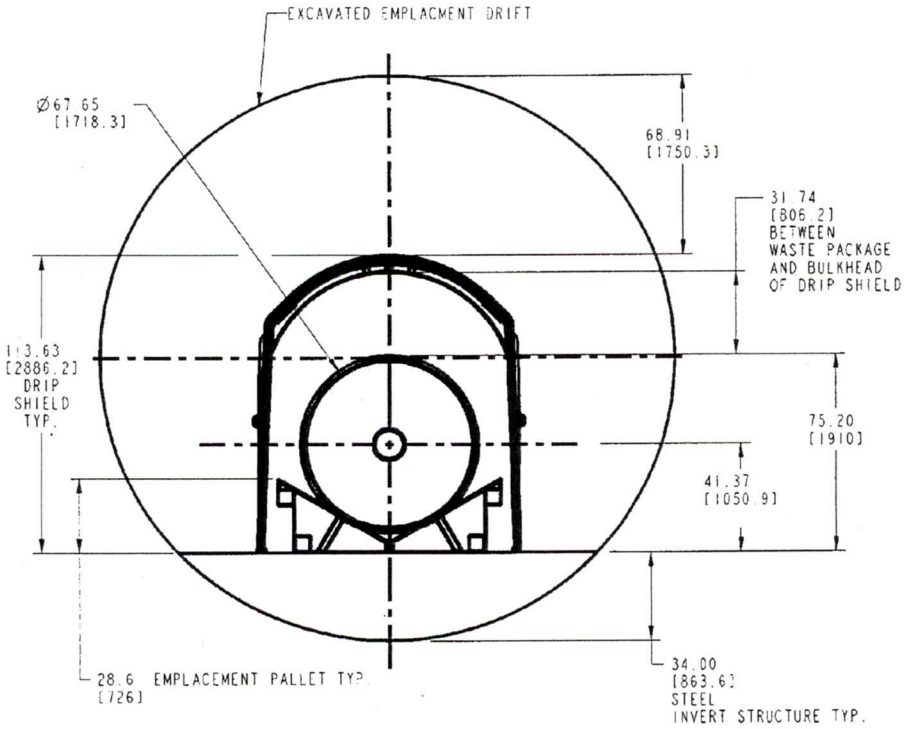

Source: BSC 2004 [DIRS 170074].

NOTE: Dimensions: inches [millimeters]; Dimensions are utilized as references only.

Figure 5-5. Configuration Inside the Emplacement Drift During the Postclosure Period

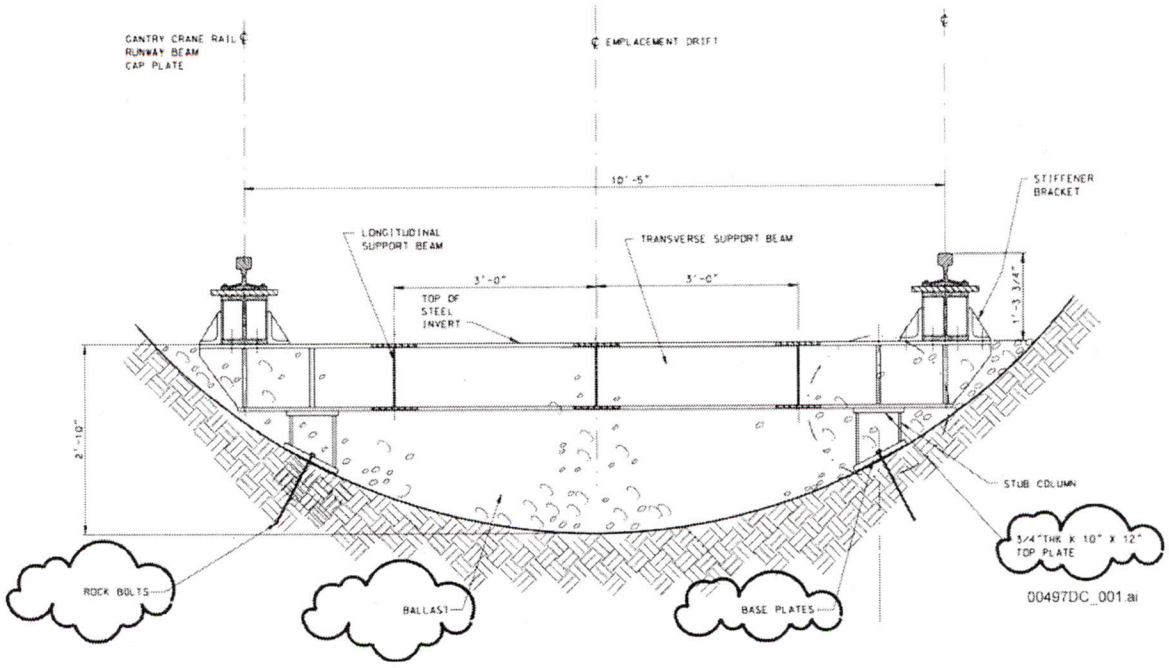

Source: BSC 2004 [DIRS 169776].

NOTE: Dimensions in feet and inches are utilized as references only.

Figure 5-6. Detail of the Steel Invert Structure and Crushed Tuff Ballast at the Bottom of the Emplacement Drift

5.2.2 Drip Shield Numerical Representation

Different numerical representations of the DS are used for the various loading conditions and analysis requirements. Because these calculations are computationally intensive (in terms of computer memory requirements and computer simulation run-time), it is necessary that the numerical representation be optimized for the particular loading case and objectives of the calculation.

Assumptions 3.16, 3.17 and 3.19 are used in development of FE representations of the DS. Assumptions 3.20 and 3.21 are used in development of DE representation. The invert is represented in all calculations as rigid. The DS is designed to be free standing on the invert, and is represented in the calculations as freely resting on the invert with a coefficient of friction between the DS footing and the invert specified as appropriate (Assumptions 3.8, 3.10 and 3.11). As illustrated in Figures 5-5 and 5-6, the only constraints to the DS motion are the drift walls, pallet and gantry rail. It is assumed (Assumption 3.16) that the gantry rail, manufactured of carbon steel, will corrode away and present no restrain to motion of the DS. Because it is assumed that the life of standard carbon steel rail is on the order of hundreds of years, this assumption is adequate for most of the duration of the regulatory period. The accumulated rockfall (due to seismic shaking or time-dependent drift degradation), if present, provides a lateral constraint to motion of the DS. Sensitivity of the calculation as a result of the presence of the lateral constraint provided by rockfall is examined in the DE kinematic analyses. The impact of lateral constraints on damage to drip shield plates under vibratory motion subsequent to the rockfall is not assessed. The largest damaged area of surface plates is predicted (Tables 5-26 and

5-27) for the vertical impact by rockfall, in which case the lateral constraints are inconsequential. It is not expected that the lateral constrain would affect significantly the results of calculations for the side impacts.

The DSC assembly, lifting feature, and base were excluded from the FE representation (Assumption 3.19) (the DSC assembly and base were included in the analysis of damage from vibratory ground motion). The benefit of this simplification is to reduce the computer execution time while preserving the features of the problem most relevant to the structural response of the DS.

5.2.2.1 Representations for Vibratory Ground Motion

An objective of this calculation was to investigate the effect of vibratory ground motion on the potential for separation of the DS and to determine the areas of residual first principal stress that exceed 50 percent of the Ti-7 yield strength (Section 5.2.3.1.4). For analysis of DS separation, it is necessary to consider motion and interaction of a large number of DSs. To conduct such an analysis using a detailed representation of the DS geometry (required for proper analysis of impact-induced damage) would be demanding computationally. Instead, two different approaches were used:

- Simplified DE kinematic calculations of motion of a large number of DSs to investigate the potential for DS separation
- FE calculation of interaction of 3 DSs (with detailed representation of the DS geometry) to analyze impact damage.

Two-dimensional DE kinematic calculations using the UDEC software (BSC 2002 [DIRS 161949]) were conducted to investigate the effect of vibratory ground motion on potential for DS separation only. Because the dominant mode of deformation of the DSs that affects their separation and interaction during seismic ground motions is their rigid body motion, the DS is represented as a rectangular (in two dimensions), deformable body with the overall DS dimensions (i.e., length, height and mass [Section 5.2.1]). Normal and shear contact relations are used to represent interaction of the DSs (Section 5.2.3.2.2.2). The DSs may become separated when limiting shear (relative vertical) displacement or limiting axial force is exceeded. If the limiting shear displacement is exceeded, the DSs become unlocked, and if the limiting axial force between two interlocked DSs is exceeded, welds of the interlocking feature are sheared and the connection is broken. The DSs will not separate as long as they move synchronously. The loss of synchronicity in DS motion is primarily a result of the following factors:

- Differential motion of the invert along the drift resulting in variable normal and shear impulse transferred to the DSs along the interconnected "chain" of DSs. If the incoming seismic wave propagates as a plane wave traveling vertically upward, all points with the same elevation move synchronously. If the incoming wave is not propagating vertically upward, there is an effect of the traveling wave along the emplacement drift that will cause a differential motion of the DSs, resulting in strain in the chain of the DSs and potential separation.

- Variability in friction coefficient (between the DS and the invert) along the chain, resulting in variable shear impulse transferred to the DSs.

- Variability of the conditions of interaction with the neighboring DSs. The DSs at the ends of the chain are always the source of the perturbation because of the asymmetric conditions of interaction—i.e., the end DS interacts with a DS on one side and is free on the other side.

The DE kinematic analysis employs a simplified representation of the DS. This analysis is supplemented by analysis of an extreme case regarding the potential for DS separation and damage due to vibratory motion impacts using a detailed FE representation of three adjacent DSs (only the central DS of those three is deformable). In this case, a rigid longitudinal boundary is assumed on both sides of the chain of three DSs. The main objective of the FE calculations is to estimate damage due to interacting impacts of adjacent DSs.

5.2.2.1.1 Representation for Kinematic Analysis

The kinematic analysis was carried out using the two-dimensional DE code UDEC. Only two components of ground motion were considered: one horizontal (along the axis of the drift) and one vertical (Assumption 3.20) applied to a longitudinal section of the drift. The lateral motion of the DSs in the plane perpendicular to the emplacement drift axis was not considered (Assumption 3.21).

Each DS is represented as a rectangular deformable body defined by 5 grid points (and 4 elements) representing the DS. Rigid-body motion is the dominant mechanism for motion and separation of the DSs within the framework of this analysis. The entire geometry of the numerical representation is discretized into elements, but the portions of the domain that represent the invert and the roof of the drift are rigid because their motion is controlled to be coincident with the input ground motion time history during the simulation. The dimensions and weight of the DS listed in Section 5.2.1 are used in the calculations. Because the DSs overlap in reality, the length of the DS in this simplified representation is reduced for the length of the overlap (i.e., BSC 2004 [DIRS 169220], 320 mm). The geometry of the DS representation in the UDEC calculation, for the case of an open emplacement drift is shown in Figure 5-7.

Numerical simulations indicate that the drifts in the lithophysal rock mass collapse completely for a PGV larger than approximately 2 m/s (BSC 2004 [DIRS 166107], Section 6.4.2.2.2). In the nonlithophysal rock mass, the amount of rockfall predicted in the drifts at this level of PGV approximately fill the region between the DS and the drift wall (BSC 2004 [DIRS 166107], Section 6.4.2.2.2). Some ground motions from the set of 1×10^{-5} ground motions and all 1×10^{-6} and 1×10^{-7} ground motions have a PGV larger than 2 m/s. It is shown in the *Drift Degradation Analysis* (BSC 2004 [DIRS 166107], Section 6.4.2.2.2) that most of the predicted rockfall takes place within about two seconds after strong ground motion begins. Different levels of rockfall (but not complete drift collapse) are predicted for ground motions with a PGV less than 2 m/s. If the drift completely collapses, the DS will be covered with at least 5 m of rubble. The rubble will also fill the space between the DS and the drift walls.

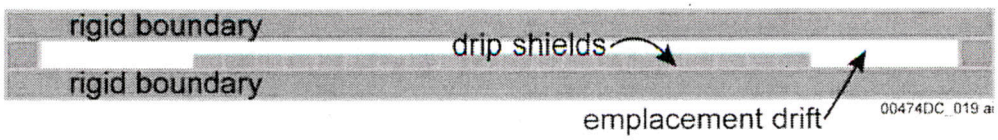

Figure 5-7. UDEC Representation of a Chain of 20 Drip Shields Linked Together at Their End Contacts

Two different approaches were used to account for the effect of the rockfall on the rigid body movement of the DS and the potential for DS separation. Sensitivity cases in which rubble covers the DS were analyzed using the geometrical representation illustrated in Figures 5-8 and 5-9. The collapsed rock that accumulates on top of the DS is represented as a layer of material of a given thickness (Young's modulus and density, see Section 5.2.3.5 on discussion of rubble properties). Different combinations of rubble properties and dimensions are analyzed (Table 5-19). In the first step of a simulation, the layer of the collapsed rock is completely unrestrained and rests on the DSs. Simulation of seismic shaking is carried out after the equilibrium stresses caused by the weight of the rubble and the DSs are generated. During the seismic shaking, the top boundary of the rubble layer is moved rigidly in synchronous motion with the far-field ground motion. In the two-dimensional analysis, the calculation is conducted for a unit thickness, i.e., 1 m in the out-of-plane direction. Although the mass of the DS representation in the UDEC calculation is 5,000 kg, which is the total mass of the DS, the pressure and reactive stresses of the caved rock are accounted for in only 1 m of the model out-of-plane thickness (the width of the DS is approximately 2.5 m). Because this approach also does not account for the frictional forces between the DS and the rubble accumulated between the DS and the drift walls, the calculations are conservative in nature.

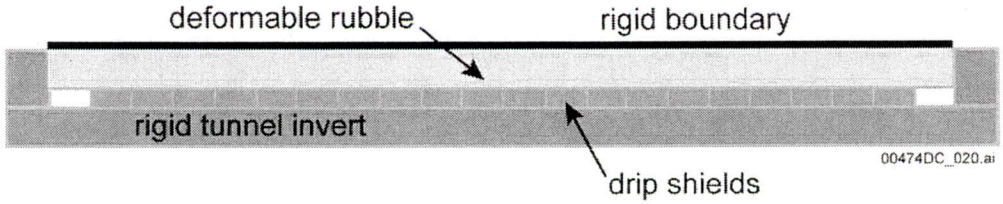

NOTE: The analysis depicted above has a simplified representation of the rubble as a coherent block of elastic material that rests on the drip shields. No rubble is represented at the ends of the DS chain.

Figure 5-8. UDEC Representation of Chain of 20 Drip Shields Covered with Rubble

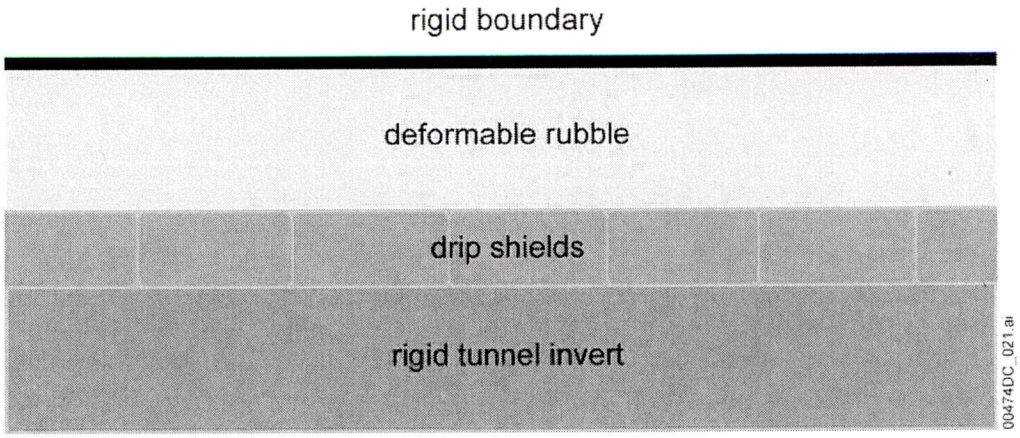

Figure 5-9. Detail of UDEC Representation of Drip Shields Covered with Rubble

The effect of the friction between the DS and the rubble on the sides of the DS (when a limited amount of rockfall does not cover the top of the DS, but rests between the DS and tunnel wall) is simulated using the geometrical representation shown in Figure 5-7. The frictional forces, applied at the 4 corners of each of the blocks that represent the DS, are calculated using the following relation:

$$F_{\text{fric}} = 0.25 f_{m\text{-}r} l_{ds} h_{ds} p_{av}, \qquad \text{(Eq. 5-1)}$$

where l_{ds} and h_{ds} are DS length and height (Section 5.2.1), f_{m-r} is the metal-to-rubble friction coefficient, and p_{av} is the average horizontal static pressure of the broken rubble. The pressure of the rubble can be estimated using the formula for the active ground pressure in cohesionless materials (e.g., Sowers 1979 [DIRS 107479], page 385, equation 9:3b):

$$p(h) = \rho_r g h \tan^2(45^\circ - \phi_r / 2), \qquad \text{(Eq. 5-2)}$$

where ρ_r is the density of the rubble, h is the height, g is gravitational acceleration, and ϕ_r is the angle of internal friction of the rubble. If the rubble height, h, is equal to the height of the DS (2,886 mm), the maximum horizontal pressure is 12,551 Pa for a typical angle of internal friction of 40 degrees (Section 5.2.3.5). The pressure varies linearly from a maximum value at the invert to zero at the top of the DS. Because the pressure is acting on both sides of the DS, the average horizontal pressure is 12,551 Pa. The force F_{fric} acts always in the direction opposite to the relative velocity between the DS and the far-field.

The parts of the calculation domain and the boundaries indicated as rigid in Figures 5-7, 5-8, and 5-9 are subjected to prescribed velocities throughout the simulations. The velocity histories are functions of the prescribed far-field velocity histories and the angle of incidence of the incoming seismic waves. The seismic waves are considered to propagate as plane (normal and shear) body waves. The effect of interactions between the seismic waves and the emplacement drifts, or any other excavations in the vicinity, is neglected.

The velocity of point x_i can be derived in the coordinate system aligned with the direction of the incident seismic wave, taking into account the phase change as a function of distance (Figure 5-10):

$$\tilde{v}_1(x_i,t)=\begin{cases}0, & \text{for } t-\dfrac{d}{C_p}\le 0\\ v_n\left(t-\dfrac{d}{C_p}\right), & \text{otherwise}\end{cases} \qquad \text{(Eq. 5-3)}$$

$$\tilde{v}_2(x_i,t)=\begin{cases}0, & \text{for } t-\dfrac{d}{C_s}\le 0\\ v_s\left(t-\dfrac{d}{C_s}\right), & \text{otherwise}\end{cases} \qquad \text{(Eq. 5-4)}$$

where $v_n(t)$ and $v_s(t)$ are prescribed vertical and horizontal velocity histories; and C_p and C_s are P- and S-wave velocities, respectively. A simple coordinate transformation was used to calculate the velocity components in the original coordinate system:

$$\begin{aligned} v_1(x_i,t) &= \tilde{v}_1(x_i,t)\sin(a_{inc})-\tilde{v}_2(x_i,t)\cos(a_{inc})\\ v_2(x_i,t) &= \tilde{v}_1(x_i,t)\sin(a_{inc})+\tilde{v}_2(x_i,t)\cos(a_{inc}) \end{aligned} \qquad \text{(Eq. 5-5)}$$

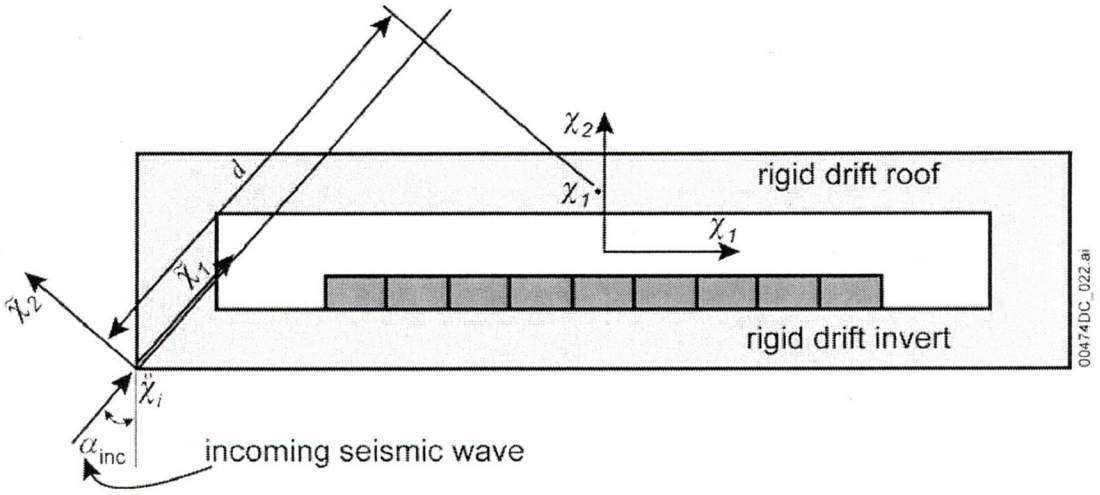

Figure 5-10. Nomenclature for Far-Field Velocity Calculation

5.2.2.1.2 Detailed Finite Element Representation

The three-dimensional FE representation, used for the vibratory ground-motion simulations, is developed in ANSYS V5.6.2, by using the DS dimensions provided in Attachment I of (BSC 2004 [DIRS 167083]). The FE representation is shown in Figure 5-11. A corresponding cutaway view (portions of various parts are removed for viewing inside the outer model boundary) is presented in Figure 5-12. As seen in these figures, the FE representation consists of three interlocking DSs, the waste package-pallet assembly, the invert surface, and the lateral and longitudinal boundaries.

Three interlocking DS's have identical geometry. However, the purpose of three interlocking DS's in the calculation is different, based on the detail to which yield mechanisms are to be represented. The finely meshed middle DS is analyzed using a bilinear elastoplastic constitutive representation for the Ti-7 and Ti-24 (Section 5.2.3.1.4). All results presented in this document are evaluated exclusively for the DS plates of the middle DS. The other two, more coarsely meshed DSs (called "peripheral DSs"), are represented as rigid (with exception of their DSC plates). The purpose of the peripheral DSs is to ensure realistic boundary conditions for the middle DS.

The boundary conditions for the DS representation used for surface plate damage are shown in Figure 5-11. The longitudinal fixed, rigid end boundary, representing the neighboring waste package pallet assemblies and DSs (which are moving synchronously with the far-field), provides constraints for the unanchored repository components in the longitudinal direction. The lateral boundary (perpendicular to the drift axis) represents the walls of the emplacement drift. The lateral and longitudinal boundaries are both rigid and fixed to the invert by tied-interface contacts (for the tied-interface contacts, LS-DYNA V960.1106, Livermore Software Technology Corporation 2001 [DIRS 159166], p. 6.29). Thus, the motion of the boundaries and the invert is completely synchronous.

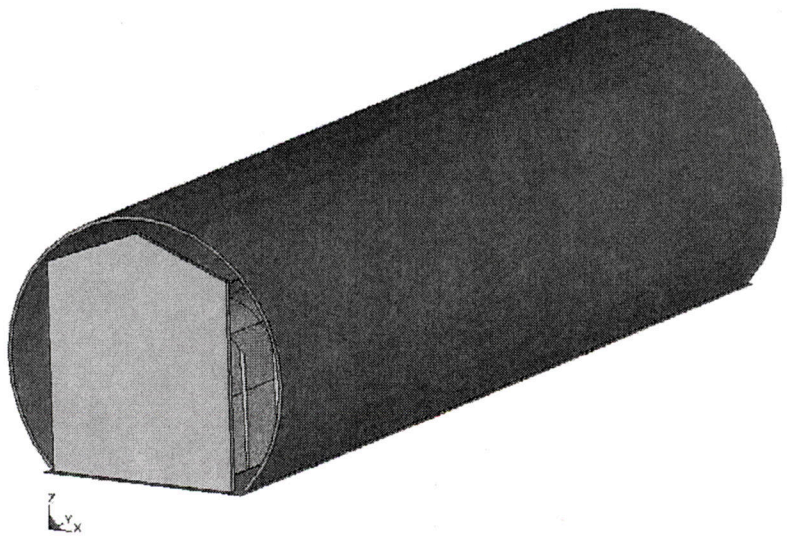

Source: BSC 2003 [DIRS 163425], Figure 1.

Figure 5-11. Setup for DS Vibratory Simulations

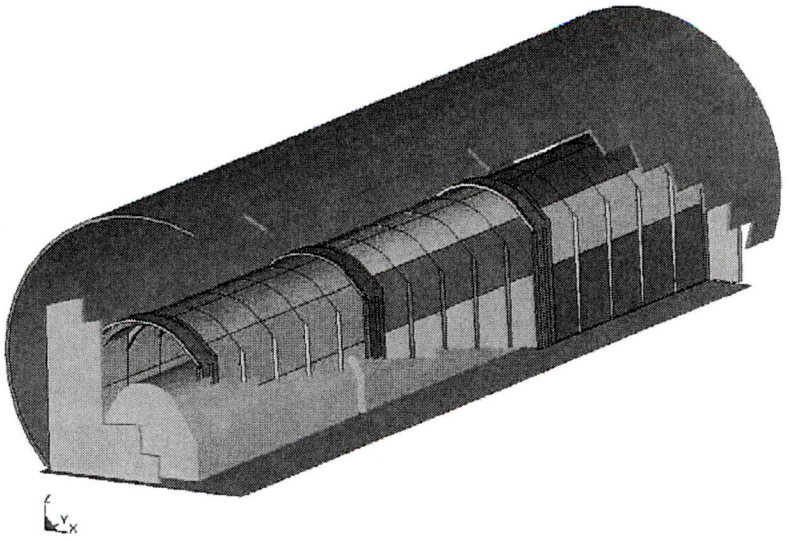

Source: BSC 2003 [DIRS 163425], Figure 2.

Figure 5-12. Cutaway View of Setup for DS Vibratory Simulations Showing Drip Shields and Internal Waste Package–Pallet Assembly

The waste package pallet assembly is a structure developed to represent the physical size, shape and mass of the waste package and pallet, but represented crudely for computational convenience. The main purpose of waste package pallet assemblies is to impose proper boundary conditions on the DSs (most importantly, the middle DS) in both a conservative (from the standpoint of the DS damaged area) and time-efficient manner. Thus, the structure of the 21-PWR waste package[7] and pallet is simplified by reducing their FE representation to a rigid thick-wall structure of uniform density (waste package pallet assembly). The geometry of the waste package pallet assembly is defined based on the contour of the waste package mounted on the pallet (Figure 5-13). The most relevant outside dimensions of the waste package mounted on the pallet are matched by FE representation and kept unchanged during the vibratory simulation (since the waste package in this FE representation cannot move relative to the pallet [see Section 5.3.2.2 for detailed discussion]). The thickness of the waste package pallet assembly is determined by using the material properties (including density) of Alloy 22, and matching the total masses of the waste package and pallet as presented in *D&E/PA/C IED Typical Waste Package Components Assembly* (BSC 2004 [DIRS 169472]) and *Emplacement Pallet* (BSC 2003 [DIRS 161520]). The initial longitudinal distance between the neighboring waste package pallet assemblies, 0.1 m, is based on the initial longitudinal distance between the neighboring waste packages (Williams 2002 [DIRS 159916], Table 2). The benefit of using this approach is to reduce the computer execution time while preserving the features of the problem most relevant to the structural response of the middle DS. (for further discussion of the waste package pallet assembly see Section 5.3.2.2.).

[7] The 21-PWR assembly is used here as it is the most common type of waste package assembly to be emplaced in the repository (roughly 38 percent – BSC 2004 [DIRS 169472], Table 11).

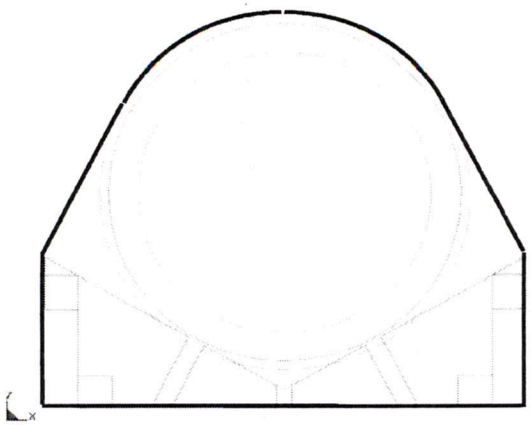

Source: BSC 2003 [DIRS 163425], Figure 3.

Figure 5-13. Contours of Waste Package Pallet Assembly and Waste Package Mounted on Pallet

Three components of the ground-motion acceleration time history are simultaneously applied on the platform representing the invert surface, which is unyielding (elastic)[8]. Externally applied momentum is transferred to all freestanding (unanchored) objects solely by friction and impact.

The DSC support beams, the DSC connector guides, the DSC guides, the support beam-connectors, the peripheral bulkheads, and the boundary walls are represented by eight-node solid (brick) elements. All other parts are represented by four-node shell elements. In general, the shell elements are adequate for representation of structural components as long as their dominant mode of deformation is bending. It is important to note that this analysis is focused on the DS plates; the stress state in other DS parts is of interest only to the extent it affects the DS plates results. The damage in other structural elements is not essential for overall performance of the DS as long as the structure remains stable. Time-dependent stress corrosion of the structural elements other than the DS plates will not significantly affect potential for water seeping through the DS on the waste packages. A possible effect of time-dependent stress corrosion would be weakening of the structure for any subsequent seismic events, but this is felt to be a second-order effect and is not analyzed here. The shell element used for representation of the DS plates is fully integrated four-node shell element with Gauss integration and five integration points through the shell thickness (Livermore Software Technology Corporation 2003 [DIRS 166841], p. 26.22). The use of shell elements in the FE representation of DS is further discussed in Section 5.3.2.1.

The FE representation is used in LS-DYNA to perform a transient dynamic analysis of the interlocking DSs exposed to vibratory ground motion. The simulation is performed in two steps. The first step is simulation of vibratory motion. During this computational phase the three components of ground-motion acceleration time history are simultaneously applied to all invert nodes. In the course of this vibratory simulation, neither system damping nor contact damping (between the unanchored objects) is applied. This conservative approach is used in order to prevent unwanted interference of the damping with the rigid-body motion of unanchored structures that could affect the results. The second step of the simulation is the post-vibratory

[8] This is a formal LS-DYNA requirement; the same acceleration time history applied to all platform nodes result in zero deformation by definition, thus, the invert is essentially rigid.

relaxation. During this computational phase the motion of the invert nodes is constrained in all three directions, and the only load applied to freestanding objects is the acceleration of gravity. In the course of this phase, the system damping is applied globally (to all objects). The goal of this step is to obtain steady-state results (and residual stresses in the DS plates) in a reasonable time, while the purpose of the global system damping is to reduce the convergence time (see Section 5.2.6 for details). The specified duration (0.5 s) of this post-vibratory relaxation part of the simulation is to allow for the steady-state stresses to equilibrate, which can be verified by visual inspection of the residual stress distributions by the post-processing graphical software program, LS-POST V2.

The mesh of the FE representation is appropriately generated and refined in appropriate regions according to standard engineering practice. This practice calls for use of finer meshing in areas of potential contact and/or stress concentration. Thus, the accuracy and representativeness of the results of this calculation are acceptable (see Section 5.2.2.4.1 for discussion of results). The uncertainties are taken into account by random sampling (from appropriate probability distributions) of the calculation inputs that are inherently stochastic (uncertain) and characterized by a large scatter of data (namely, ground-motion time histories and friction coefficients as discussed in more detail in Section 5.3.1.2).

5.2.2.2 Finite Element Representation for Rock Impact in Nonlithophysal Rock Mass

The objective of this calculation is to determine the DS damaged areas after impact by rockfall in nonlithophysal rock mass (Section 1). These areas are calculated using the postprocessor LS-PREPOST V1.0, and verified by visual inspection and measurement of the FE representation.

The three-dimensional FE mesh representations of the DS and the impacting rock blocks are developed in ANSYS V5.6.2 for six different rock sizes. Based on the nonlithophysal rockfall estimates presented in *Drift Degradation Analysis* (BSC 2004 [DIRS 168550], Section 6.3), three different rockfall-DS impact orientations have been considered: vertical, DS corner, and DS side-wall (described in Section 5.4.2.1). The FE representations of the DS are developed by using the dimensions provided in *Drip Shield Structural Response to Rock Fall* (BSC 2004 [DIRS 168993], Attachment I).

All of the DS components are represented by constant stress eight-node solid (brick) elements (Livermore Software technology Corporation 2003 [DIRS 166841], p. 26.30). One-point Gaussian quadrature is used for the solid element (Hallquist 1998 [DIRS 155373], Section 3). Because the DS top plate and the side-walls are the most important DS components in this calculation, all damaged areas are reported exclusively for these parts. To capture the details of stress concentration at the rock block impact location, the FE representation of the DS consists of one finely-meshed region where rock impact takes place, and coarsely-meshed regions elsewhere. The FE representation of the DS top plate has five layers of brick elements through the thickness. Furthermore, the FE mesh is refined in the impact regions in both axial and circumferential directions. The geometry of the FE representations used in this calculation is illustrated in Figures 5-14 and 5-15.